Depth of diamond formation obtained from single periclase inclusions

Chiara Anzolini[1]*, Fabrizio Nestola[1], Mattia L. Mazzucchelli[2], Matteo Alvaro[2], Paolo Nimis[1], Andrea Gianese[1], Simone Morganti[3], Federica Marone[4], Marcello Campione[5], Mark T. Hutchison[6], and Jeffrey W. Harris[7]

[1]Department of Geosciences, University of Padova, Via G. Gradenigo 6, 35131 Padua, Italy
[2]Department of Earth and Environmental Sciences, University of Pavia, Via A. Ferrata 1, 27100 Pavia, Italy
[3]Department of Electrical, Computer, and Biomedical Engineering, University of Pavia, Via A. Ferrata 5, 27100 Pavia, Italy
[4]Swiss Light Source, Paul Scherrer Institut, 5232 Villigen, Switzerland
[5]Department of Earth and Environmental Sciences, University of Milano Bicocca, Piazza della Scienza 4, 20126 Milan, Italy
[6]Trigon GeoServices Ltd., 2780 South Jones Blvd, Suite 35-15, Las Vegas, Nevada 89146, USA
[7]School of Geographical and Earth Sciences, University of Glasgow, G12 8QQ Glasgow, UK

ABSTRACT

Super-deep diamonds (SDDs) are those that form at depths between ~300 and ~1000 km in Earth's mantle. They compose only 1% of the entire diamond population but play a pivotal role in geology, as they represent the deepest direct samples from the interior of our planet. Ferropericlase, (Mg,Fe)O, is the most abundant mineral found as inclusions in SDDs and, when associated with low-Ni enstatite, which is interpreted as retrogressed bridgmanite, is considered proof of a lower-mantle origin. As this mineral association in diamond is very rare, the depth of formation of most ferropericlase inclusions remains uncertain. Here we report geobarometric estimates based on both elasticity and elastoplasticity theories for two ferropericlase inclusions, not associated with enstatite, from a single Brazilian diamond. We obtained a minimum depth of entrapment of 15.7 (±2.5) GPa at 1830 (±45) K (~450 [±70] km depth), placing the origin of the diamond-inclusion pairs at least near the upper mantle–transition zone boundary and confirming their super-deep origin. Our analytical approach can be applied to any type of mineral inclusion in diamond and is expected to allow better insights into the depth distribution and origin of SDDs.

INTRODUCTION

Diamonds, and the mineral inclusions they trap during their growth, are pristine samples from Earth's mantle and provide information on processes operating in inaccessible regions of our planet. This information is particularly valuable if it can be combined with depth estimates. Based on the mineral inclusions, the majority of diamonds (99%) originate within the lithosphere (Stachel and Harris, 2008). The other 1% are sublithospheric and formed at depths between ~300 and ~1000 km, and hence are called super-deep diamonds (SDDs) (Walter et al., 2011; Pearson et al., 2014; Smith et al., 2016; Nestola et al., 2018).

Based on experimental evidence, bridgmanite and ferropericlase are the most abundant minerals in the lower mantle, composing approximately ~75 and ~17 wt%, respectively (Stixrude and Lithgow-Bertelloni, 2012, and references therein). On decompression, bridgmanite inverts to Al-rich, low-Ni enstatite (Stachel et al., 2000), while ferropericlase can remain stable to room pressure. Numerous lines of evidence, particularly

association with low-Ni enstatite, have indicated that ferropericlase has a lower-mantle origin (Harte et al., 1999; Stachel et al., 2000). However, the association of ferropericlase with olivine and jeffbenite (previously known as TAPP; Nestola et al., 2016) (Hutchison et al., 2001) casts doubt on that conclusion. Indeed, ringwoodite is in equilibrium with ferropericlase at 24 GPa (Brey et al., 2004) and could have later reverted to olivine, whereas jeffbenite is stable only up to 13 GPa (Armstrong and Walter, 2012), even as its origin is still controversial. In addition, the observation of droplets of Fe-Ni alloys in some Fe-enriched ferropericlases induced Hayman et al. (2005) to outline a model that ascribes the Fe-rich character to equilibration with silicates in the deeper part of the lower mantle (1700–2900 km). On the other hand, synthesis of ferropericlase and diamond by carbonate melt–peridotite reactions (Thomson et al., 2016) suggested that ferropericlase inclusions with variable Fe contents can form at lower upper-mantle to transition-zone depths. The presence of nanometric exsolutions of magnesioferrite in some ferropericlase inclusions (Harte et al., 1999; Wirth et al., 2014; Kaminsky et al., 2015) led Palot et al. (2016) to propose an origin in the uppermost part of the lower mantle, but Uenver-Thiele et al. (2017a, 2017b) showed that magnesioferrite cannot exsolve directly from ferropericlase in the lower mantle.

In aiming to identify a method for determining the depth of origin of ferropericlase inclusions completely independent of mineral paragenesis, Hutchison (1997) combined sophisticated thermoelastic modeling with measurements of periclase cell parameters before and after release from diamonds from the São Luiz River (Juina, Brazil) and Guinea. Hutchison and Harris (1998) reported an absolute minimum depth of formation of 320 km (equivalent to an entrapment pressure, P_{trap}, of 11 GPa), uncorrected for the brittle deformation evident in the diamond host. This study provided strong evidence for super-deep origins for the samples analyzed, however limitations were imposed by uncertainties in the Gandolfi camera measurement technique available at the time and full quantification of plastic and brittle diamond deformation. In this study, we have been able to extend the original work with improved certainty and propose an updated method for determining minimum P_{trap} applied to two ferropericlase inclusions in a further diamond from the São Luiz River (sample AZ1; Fig. 1). The reverse calculation of P_{trap} was performed by applying the elastic geobarometry

Figure 1. Inclusion-bearing diamond studied in this work (dodecahedron recovered from alluvial deposits of the São Luiz River, in the Juina area of Mato Grosso State, Brazil). Inclusions studied are indicated with arrows.

approach (Angel et al., 2015a, 2015b, 2017), including the full geometry of the inclusions based on a realistic three-dimensional (3-D) reconstruction (Mazzucchelli et al., 2018), coupled with a new elastoplastic model to account for plasticity of the diamond host at high temperature.

METHODS

Sample

The diamond investigated in this study (Fig. 1) is a flattened colorless dodecahedron recovered from alluvial deposits of the São Luiz River, in the Juina area of Mato Grosso State, Brazil (see also Harte et al., 1999; Hayman et al., 2005; Kaminsky et al., 2015). The sample contains two main black tabular inclusions, identified as ferropericlase [$(Mg_{0.60}Fe_{0.40})O$; see below] by single-crystal X-ray diffraction (see the GSA Data Repository[1]). The smaller inclusion, whose longest dimension is ~160 μm, is named AZ1_1; the larger one, whose longest dimension is ~340 μm, is named AZ1_2.

Synchrotron X-ray Tomographic Microscopy

Synchrotron X-ray tomographic microscopy is a non-destructive, high-resolution technique that creates 3-D maps of the variations of the X-ray attenuation coefficient within a sample. X-ray microtomography experiments were carried out at the Swiss Light Source (SLS; Paul Scherrer Institut, Switzerland) at TOMCAT, a beamline for tomographic microscopy and coherent radiology experiments (Stampanoni et al., 2006).
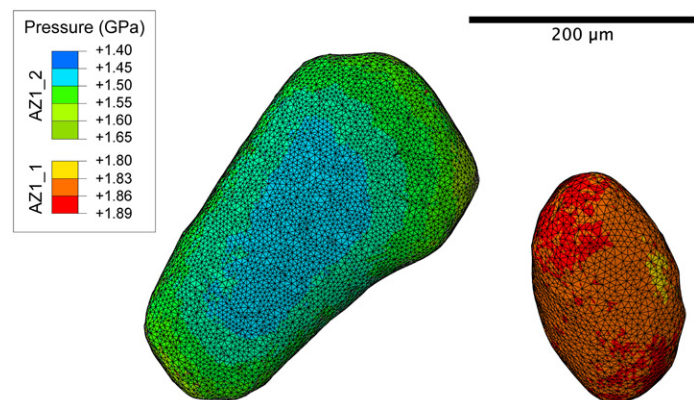

Figure 2. Three-dimensional model of ferropericlase inclusions (AZ1_1 and AZ1_2) in studied diamond (dodecahedron recovered from alluvial deposits of the São Luiz River, in the Juina area of Mato Grosso State, Brazil), built from segmentation of X-ray microtomographic data set. It preserves morphology of both inclusions and their mutual distances and orientations, and reveals absence of significant fractures around inclusions. Pressure calculated by finite element analysis is not homogeneous within inclusions. Final residual pressures (P_{inc}) reported in text are obtained for each inclusion as average of pressure over their entire volume and include also uncertainty in calculation.

Measurements were performed at 13.5 keV in order to maximize contrast. A total of 1501 X-ray radiographs were acquired from different angular positions around a vertical rotation axis for each sample. The imaging setup consisted of a 20-μm-thick LuAG:Ce scintillator screen, a 20× objective, and a scientific complementary metal-oxide semiconductor (CMOS) camera (PCO.edge). The tomographic reconstruction was performed using optimized routines based on the Fourier transform method (Marone and Stampanoni, 2012). The resulting volume consisted of 2160 axial slices of 2560 × 2560 pixels, with a pixel size of 0.33 μm.

Single-Crystal X-ray Diffraction (SCXRD)

SCXRD measurements were performed on the ferropericlase inclusions both before and after release from their diamond host at the Department of Geosciences, University of Padova (Italy). X-ray data were collected using a Rigaku Oxford Diffraction SuperNova single-crystal diffractometer, equipped with a Dectris Pilatus 200 K area detector and with a Mova X-ray microsource. A monochromatized Mo$K\alpha$ radiation ($\lambda = 0.71073$ Å), working at 50 kV and 0.8 mA, was used. The sample-to-detector distance was 68 mm. Data reduction was performed using the CrysAlisPro software (Rigaku Oxford Diffraction; https://www.rigaku.com/en/products/smc/crysalis).

Field Emission Gun–Scanning Electron Microscopy (FEG-SEM)

The two ferropericlase inclusions were first extracted by mechanical crushing of the host, then polished in a three-step process, and finally carbon coated. FEG-SEM measurements were carried out at the Department of Physics and Astronomy, University of Padova, using a Zeiss Sigma HD FEG-SEM microscope operating at 20 kV, with a spot size of ~1 nm. Imaging was performed using an InLens secondary electron detector. Compositional analysis was performed using an energy dispersive X-ray spectrometer (EDX by Oxford Instruments). The spatial resolution in microanalysis was ~1 μm.

Finite Element (FE) analysis

The FE analysis was performed on the real 3-D model built from the segmentation of the X-ray microtomographic data (Fig. 2). The surface of the model was smoothed to improve the quality of the final FE mesh, and the final 3-D model was then assembled, placing the two inclusions in the diamond host. The full procedure is reported in the Data Repository.

Elastoplastic Model

The calculation is split into an isothermal, quasi-static decompression from entrapment conditions (P_{trap} and T_{trap}; T is temperature) to P_{room} and T_{trap}, followed by an isobaric cooling to room temperature (see Campione, 2018). This is assumed to be a realistic approximation of the P-T path experienced by diamonds exhumed to the Earth's surface through kimberlite pipes. For further details, see the Data Repository.

RESULTS AND DISCUSSION

Sample Analysis

The 3-D reconstruction (Fig. 2) revealed the absence of significant fractures at inclusion terminations. However, graphitization in haloes around the inclusions (Fig. 1) suggests that some pressure release by brittle deformation of the host diamond may have occurred. Both inclusions, after release and polishing, exhibited pervasively and homogeneously distributed exsolutions of magnesioferrite of ~200 nm size, which commonly coalesced into chains of 2–3 μm length and constituted ~6% of the total surface area (calculated using ImageJ software; Abràmoff et al., 2004). EDX analyses gave a composition of $(Mg_{0.61}Fe_{0.39})O$ for inclusion AZ1_1 and $(Mg_{0.59}Fe_{0.41})O$ for AZ1_2; therefore, we consider them to have a similar approximate composition of $(Mg_{0.60}Fe_{0.40})O$ (Fig. DR1 in the Data Repository).

Inclusion Residual Pressures

X-ray analyses (Fig. DR2) provided the lattice parameters and the relative unit-cell volumes reported in Table DR1 in the Data Repository. By comparing the unit-cell volumes before (V) and after (V_0) release from the diamond host and using the P-V-T Equation of State (EoS) for ferropericlase refitted from the original data of Mao et al. (2011) (see the Data Repository), we obtained a residual pressure, P_{inc}, of 1.84 (±0.65) GPa for inclusion AZ1_1 and of 1.48 (±0.67) GPa for inclusion AZ1_2. The high uncertainties in P_{inc} are due to the high uncertainty in the bulk modulus value of ferropericlase (Mao et al., 2011). Values of P_{inc} are consistent with 1.29 (±0.38) GPa for the Guinean diamond of Hutchison and Harris (1998), where in this latter case, the uncertainty is confined to that of measurement of cell parameters.

Determination of Depth of Formation of the Ferropericlase-Diamond Pair by Elastoplastic Geobarometry

Given the absence of significant fracture systems around the inclusions, the calculated P_{inc} can be linked to the depth of formation by elastic geobarometry. Standard elastic methods rely on simplified models that assume that the inclusion is spherical and sitting isolated in an infinitely large host (e.g., Zhang, 1998). Mazzucchelli et al. (2018) showed that platy inclusions develop a lower P_{inc} compared to more rounded inclusions. This is consistent with our measurements, which show a lower P_{inc} for the platy inclusion AZ1_2 than for the more rounded AZ1_1. The method of Mazzucchelli et al. (2018) enabled us to calculate the appropriate geometrical correction factor (Γ) for the two inclusions through an integration over their entire volumes. The Γ factors, calculated using the elastic properties for ferropericlase and diamond reported in the Data Repository, are –0.016 (±0.005) and –0.080 (±0.010) for inclusions AZ1_1 and AZ1_2, respectively. Applying the correction factor to our experimentally determined residual pressures, we obtained the corrected P_{inc} of 1.87 (±0.66) GPa and 1.61 (±0.73) GPa for the inclusions, respectively.

We then calculated the entrapment isomeke for the two ferropericlase-diamond pairs using the corrected values for P_{inc} and the software EosFit-Pinc (Angel et al., 2017). Because both the host and the inclusions have cubic crystallographic symmetry, the effect of anisotropic elasticity is limited (see Anzolini et al., 2018), allowing the use of current isotropic elastic geobarometry models. To keep consistency among each step of the calculation, we applied the same elastic properties used to obtain the geometrical correction factors. The intersection of the isomeke with the mantle adiabat, accounting for the isomeke and the adiabatic uncertainties, gave an entrapment pressure for inclusion AZ1_1 of P_{trap} = 13.5 (±1.8) GPa at a temperature T_{trap} = 1802 (±60) K, and for AZ1_2 of P_{trap} = 12.8 (±1.8) GPa at a temperature T_{trap} = 1794 (±60) K (see Table DR2; Fig. 3).

This estimate does not take into account plastic deformation in the diamond, which may have accommodated part of the inclusion expansion during uplift to surface (Anzolini et al., 2016). Plastic deformation is well documented in diamond and particularly in SDDs (e.g., Cayzer et al., 2008), consistent with its low yield strength (σ_Y) at high temperatures (Weidner et al., 1994). Therefore, the P_{trap} calculated from a purely elastic model is likely to be underestimated. To account for plastic deformation, an elastoplastic (EP) model (see Methods and the Data Repository) was applied. The reverse calculation of $P_{trap-EP}$ as a function of T was solved by adjusting the σ_Y of diamond according to the experimental measurements of Weidner et al. (1994) and the elastic parameters for diamond and ferropericlase. Because the EP model assumes that the inclusion is spherical, we applied this method only to the most rounded of the two inclusions, i.e., AZ1_1. The best agreement between the calculated $P_{trap-EP}(T)$ and the adiabat, with its uncertainty, is at 15.7 (±2.5) GPa and 1830 (±45) K (~450 [±70] km depth). Considering the uncertainties, this result is compatible with an origin in the lowermost upper mantle or, more probably, in the upper transition zone (Fig. 3). Unfortunately, the depth obtained is constrained by a lack of experimental values of σ_Y when temperatures are higher than
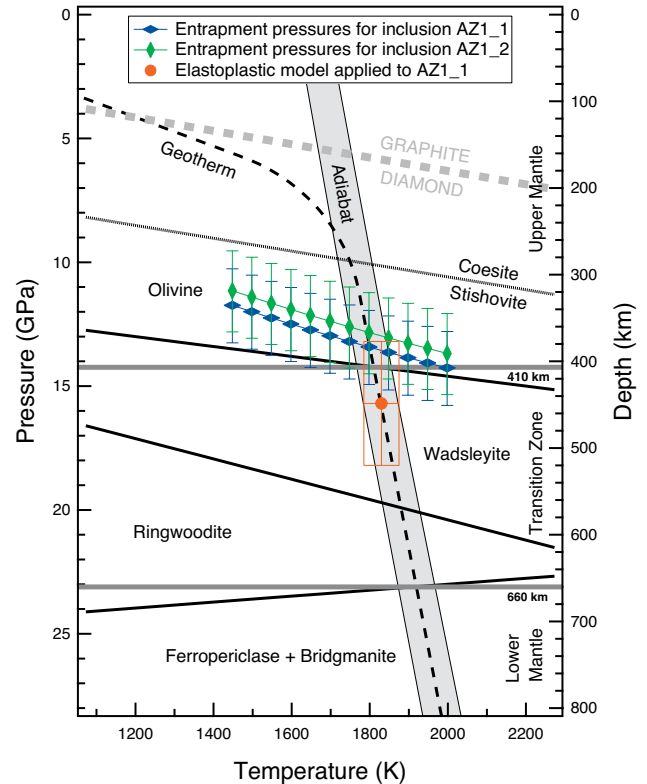

Figure 3. Minimum entrapment pressures of ferropericlase inclusions in studied diamond (dodecahedron recovered from alluvial deposits of the São Luiz River, in the Juina area of Mato Grosso State, Brazil), determined by elastic and elastoplastic (EP) models. Geotherm is calculated for typical cratonic surface heat flow of 40 mW/m² (Hasterok and Chapman, 2011) and mantle adiabat (Katsura et al., 2010; Trubitsyn and Trubitsyna, 2015). Entrapment pressures (P_{trap}) calculated for inclusions AZ1_1 and AZ1_2 at various temperatures (T) with purely elastic model are represented by blue and green diamonds, respectively. $P_{trap-EP}$ calculated with elastoplastic model for inclusion AZ1_1 at T consistent with adiabat, and its uncertainty, is represented by orange box.

~1850 K (Weidner et al., 1994) and the fact that the EP model only considers the deformation caused by overpressurization of the inclusion with respect to the external lithostatic pressure (Campione, 2018). If external tectonic stresses act on diamonds during uplift through the sublithospheric mantle, they may promote additional plastic deformation, which may contribute to the release of part of the P_{inc} being built on the inclusion. Therefore, the $P_{trap-EP}$ value of 15.7 (±2.5) GPa for AZ1_1, which corresponds to a depth of ~450 (±70) km, should be regarded as a minimum estimate.

In addition, models used in this work do not take into account the effect that the magnesioferrite exsolutions (see the Data Repository) may have on P_{inc} and, in turn, on the calculated P_{trap}. However, given the small contrast in elastic properties between ferropericlase and magnesioferrite (Reichmann and Jacobsen, 2004) and the small volume ratio (~6%) between these two minerals, the effect is probably limited and well within the uncertainties already accounted for in the calculations.

CONCLUSIONS

Our newly devised method for inclusion barometry, which incorporates an elastoplastic treatment of the inclusion-host system and a correction for geometrical effects based on a real 3-D model, can be extended to several other types of inclusions trapped in SDDs. Our analyses demonstrate that for the ferropericlase samples studied, an origin much shallower than the transition zone (Thomson et al., 2016) can certainly be excluded. Although the present results may only provide minimum pressure estimates, they yield valuable constraints independent of mineral phase relations on the depth of

origin of SDDs and thereby increase our knowledge of those inaccessible regions that play a key role in the Earth's dynamics and deep carbon cycle.

REFERENCES CITED
Abràmoff, M.D., Magalhães, P.J., and Ram, S.J., 2004, Image processing with ImageJ: Biophotonics International, v. 11, p. 36–42.

Angel, R.J., Alvaro, M., Nestola, F., and Mazzucchelli, M.L., 2015a, Diamond thermoelastic properties and implications for determining the pressure of formation of diamond-inclusion systems: Russian Geology and Geophysics, v. 56, p. 211–220, https://doi.org/10.1016/j.rgg.2015.01.014.

Angel, R.J., Nimis, P., Mazzucchelli, M.L., Alvaro, M., and Nestola, F., 2015b, How large are departures from lithostatic pressure? Constraints from host-inclusion elasticity: Journal of Metamorphic Geology, v. 33, p. 801–813, https://doi.org/10.1111/jmg.12138.

Angel, R.J., Mazzucchelli, M.L., Alvaro, M., and Nestola, F., 2017, EosFit-Pinc: A simple GUI for host-inclusion elastic thermobarometry: The American Mineralogist, v. 102, p. 1957–1960, https://doi.org/10.2138/am-2017-6190.

Anzolini, C., Angel, R.J., Merlini, M., Derzsi, M., Tokár, K., Milani, S., Krebs, M.Y., Brenker, F.E., Nestola, F., and Harris, J.W., 2016, Depth of formation of CaSiO$_3$-walstromite included in super-deep diamonds: Lithos, v. 265, p. 138–147, https://doi.org/10.1016/j.lithos.2016.09.025.

Anzolini, C., Prencipe, M., Alvaro, M., Romano, C., Vona, A., Lorenzon, S., Smith, E.M., Brenker, F.E., and Nestola, F., 2018, Depth of formation of super-deep diamonds: Raman barometry of CaSiO$_3$-walstromite inclusions: The American Mineralogist, v. 103, p. 69–74, https://doi.org/10.2138/am-2018-6184.

Armstrong, L.S., and Walter, M.J., 2012, Tetragonal almandine pyrope phase (TAPP): Retrograde Mg-perovskite from subducted oceanic crust?: European Journal of Mineralogy, v. 24, p. 587–597, https://doi.org/10.1127/0935-1221/2012/0024-2211.

Brey, G.P., Bulatov, V., Girnis, A., Harris, J.W., and Stachel, T., 2004, Ferropericlase—A lower mantle phase in the upper mantle: Lithos, v. 77, p. 655–663, https://doi.org/10.1016/j.lithos.2004.03.013.

Campione, M., 2018, Threshold effects for the decrepitation and stretching of fluid inclusions: Journal of Geophysical Research: Solid Earth, v. 123, p. 3539–3548, https://doi.org/10.1029/2018JB015694.

Cayzer, N.J., Odake, S., Harte, B., and Kagi, H., 2008, Plastic deformation of lower mantle diamonds by inclusion phase transformations: European Journal of Mineralogy, v. 20, p. 333–339, https://doi.org/10.1127/0935-1221/2008/0020-1811.

Harte, B., Harris, J.W., Hutchison, M.T., Watt, G.R., and Wilding, M.C., 1999, Lower mantle mineral associations in diamonds from São Luiz, Brazil, in Fei, Y., et al., eds., Mantle Petrology: Field Observations and High-Pressure Experimentation: A Tribute to Francis R. (Joe) Boyd: Geochemical Society Special Publication 6, p. 125–153.

Hasterok, D., and Chapman, D.S., 2011, Heat production and geotherms for the continental lithosphere: Earth and Planetary Science Letters, v. 307, p. 59–70, https://doi.org/10.1016/j.epsl.2011.04.034.

Hayman, P.C., Kopylova, M.G., and Kaminsky, F.V., 2005, Lower mantle diamonds from Rio Soriso (Juina area, Mato Grosso, Brazil): Contributions to Mineralogy and Petrology, v. 149, p. 430–445, https://doi.org/10.1007/s00410-005-0657-8.

Hutchison, M.T., 1997, Constitution of the deep transition zone and lower mantle shown by diamonds and their inclusions [Ph.D. thesis]: Edinburgh, University of Edinburgh, 660 p., http://www.trigon-gs.com/Hutchison_97.pdf.

Hutchison, M.T., and Harris, J.W., 1998, Thermoelastic interpretation of internal pressure imposed on an (Mg,Fe)O inclusion in diamond: Support for a deep mantle origin: Abstract T32G-06 presented at 1998 Fall Meeting, American Geophysical Union, San Francisco, California, 6–10 December, http://www.trigon-gs.com/Hutchison_and_Harris_98.pdf.

Hutchison, M.T., Hursthouse, M.B., and Light, M.E., 2001, Mineral inclusions in diamonds: Associations and chemical distinctions around the 670-km discontinuity: Contributions to Mineralogy and Petrology, v. 142, p. 119–126, https://doi.org/10.1007/s004100100279.

Kaminsky, F.V., Ryabchikov, I.D., McCammon, C.A., Longo, M., Abakumov, A.M., Turner, S., and Heidari, H., 2015, Oxidation potential in the Earth's lower mantle as recorded by ferropericlase inclusions in diamond: Earth and Planetary Science Letters, v. 417, p. 49–56, https://doi.org/10.1016/j.epsl.2015.02.029.

Katsura, T., Yoneda, A., Yamazaki, D., Yoshino, T., and Ito, E., 2010, Adiabatic temperature profile in the mantle: Physics of the Earth and Planetary Interiors, v. 183, p. 212–218, https://doi.org/10.1016/j.pepi.2010.07.001.

Mao, Z., Lin, J., Liu, J., and Prakapenka, V.B., 2011, Thermal equation of state of lower-mantle ferropericlase across the spin crossover: Geophysical Research Letters, v. 38, L23308, https://doi.org/10.1029/2011GL049915.

Marone, F., and Stampanoni, M., 2012, Regridding reconstruction algorithm for real-time tomographic imaging: Journal of Synchrotron Radiation, v. 19, p. 1029–1037, https://doi.org/10.1107/S0909049512032864.

Mazzucchelli, M.L., Burnley, P., Angel, R.J., Morganti, S., Domeneghetti, M.C., Nestola, F., and Alvaro, M., 2018, Elastic geothermobarometry: Corrections for the geometry of the host-inclusion system: Geology, v. 46, p. 231–234, https://doi.org/10.1130/G39807.1.

Nestola, F., Burnham, A.D., Peruzzo, L., Tauro, L., Alvaro, M., Walter, M.J., Gunter, M., Anzolini, C., and Kohn, S.C., 2016, Tetragonal Almandine-Pyrope Phase, TAPP: Finally a name for it, the new mineral jeffbenite: Mineralogical Magazine, v. 80, p. 1219–1232, https://doi.org/10.1180/minmag.2016.080.059.

Nestola, F., et al., 2018, CaSiO$_3$-perovskite in diamond indicates the recycling of oceanic crust into the lower mantle: Nature, v. 555, p. 237–241, https://doi.org/10.1038/nature25972.

Palot, M., Jacobsen, S.D., Townsend, J.P., Nestola, F., Marquardt, K., Miyajima, N., Harris, J.W., Stachel, T., McCammon, C.A., and Pearson, D.G., 2016, Evidence for H$_2$O-bearing fluids in the lower mantle from diamond inclusion: Lithos, v. 265, p. 237–243, https://doi.org/10.1016/j.lithos.2016.06.023.

Pearson, D.G., et al., 2014, Hydrous mantle transition zone indicated by ringwoodite included within diamond: Nature, v. 507, p. 221–224, https://doi.org/10.1038/nature13080.

Reichmann, H.J., and Jacobsen, S.D., 2004, High-pressure elasticity of a natural magnesioferrite crystal: The American Mineralogist, v. 89, p. 1061–1066, https://doi.org/10.2138/am-2004-0718.

Smith, E.M., Shirey, S.B., Nestola, F., Bullock, E.S., Wang, J.H., Richardson, S.H., and Wang, W.Y., 2016, Large gem diamonds from metallic liquid in Earth's deep mantle: Science, v. 354, p. 1403–1405, https://doi.org/10.1126/science.aal1303.

Stachel, T., and Harris, J.W., 2008, The origin of cratonic diamonds—Constraints from mineral inclusions: Ore Geology Reviews, v. 34, p. 5–32, https://doi.org/10.1016/j.oregeorev.2007.05.002.

Stachel, T., Harris, J.W., Brey, G.P., and Joswig, W., 2000, Kankan diamonds (Guinea) II: Lower mantle inclusion parageneses: Contributions to Mineralogy and Petrology, v. 140, p. 16–27, https://doi.org/10.1007/s004100000174.

Stampanoni, M., et al., 2006, Trends in synchrotron-based tomographic imaging: The SLS experience, in Bonse, U., ed., Developments in X-Ray Tomography V: International Society for Optics and Photonics (SPIE) Proceedings Volume 6318, 63180M, https://doi.org/10.1117/12.679497.

Stixrude, L., and Lithgow-Bertelloni, C., 2012, Geophysics of chemical heterogeneity in the mantle: Annual Review of Earth and Planetary Sciences, v. 40, p. 569–595, https://doi.org/10.1146/annurev.earth.36.031207.124244.

Thomson, A.R., Walter, M.J., Kohn, S.C., and Brooker, R.A., 2016, Slab melting as a barrier to deep carbon subduction: Nature, v. 529, p. 76–79, https://doi.org/10.1038/nature16174.

Trubitsyn, V.P., and Trubitsyna, A.P., 2015, Effects of compressibility in the mantle convection equations: Izvestiya: Physics of the Solid Earth, v. 51, p. 801–813, https://doi.org/10.1134/S1069351315060129.

Uenver-Thiele, L., Woodland, A.B., Boffa Ballaran, T., Miyajima, N., and Frost, D.J., 2017a, Phase relations of MgFe$_2$O$_4$ at conditions of the deep upper mantle and transition zone: The American Mineralogist, v. 102, p. 632–642, https://doi.org/10.2138/am-2017-5871.

Uenver-Thiele, L., Woodland, A.B., Boffa Ballaran, T., Miyajima, N., and Frost, D.J., 2017b, Phase relations of Fe-Mg spinels including new high-pressure post-spinel phases and implications for natural samples: The American Mineralogist, v. 102, p. 2054–2064, https://doi.org/10.2138/am-2017-6119.

Walter, M.J., Kohn, S.C., Araujo, D., Bulanova, G.P., Smith, C.B., Gaillou, E., Wang, J., Steele, A., and Shirey, S.B., 2011, Deep mantle cycling of oceanic crust: Evidence from diamonds and their mineral inclusions: Science, v. 334, p. 54–57, https://doi.org/10.1126/science.1209300.

Weidner, D.J., Wang, Y., and Vaughan, M.T., 1994, Strength of diamond: Science, v. 266, p. 419–422, https://doi.org/10.1126/science.266.5184.419.

Wirth, R., Dobrzhinetskaya, L., Harte, B., Schreiber, A., and Green, H.W., 2014, High-Fe (Mg,Fe)O inclusion in diamond apparently from the lowermost mantle: Earth and Planetary Science Letters, v. 404, p. 365–375, https://doi.org/10.1016/j.epsl.2014.08.010.

Zhang, Y., 1998, Mechanical and phase equilibria in inclusion-host systems: Earth and Planetary Science Letters, v. 157, p. 209–222, https://doi.org/10.1016/S0012-821X(98)00036-3.

Printed in USA